ELSEVIER

Biophysical Chemistry 58 (1996) 3–12

Biophysical Chemistry

Fluorescence correlation spectrometry of the interaction kinetics of tetramethylrhodamin α-bungarotoxin with *Torpedo californica* acetylcholine receptor

Barbara Rauer [a], Eberhard Neumann [a,*], Jerker Widengren [b], Rudolf Rigler [*,b]

[a] *Faculty of Chemistry, University of Bielefeld, P.O. Box 100 131, D-33501 Bielefeld, Germany*
[b] *Department of Medical Biophysics, Karolinska Institutet S-17177 Stockholm, Sweden*

Received 27 December 1994; revised 16 March 1995; accepted 28 March 1995

Abstract

Fluorescence correlation spectroscopy (FCS) is suited to determine low concentrations (10^{-8} M) of slowly interacting molecules with different translational diffusion coefficients on the level of single molecule counting. This new technique was applied to characterize the interaction dynamics of tetramethylrhodamin labelled α-bungarotoxin (B*) with the detergent solubilized nicotinic acetylcholine receptor (AChR) of *Torpedo californica* electric organ. At pseudo-first-order conditions for AChR, the complex formation with B* is monophasic. The association rate coefficient of the monoliganded species AChR · B is $k'_{ass} = 3.8 \cdot 10^3\ s^{-1}$ at 293 K (20°C). The dissociation of bound B* from the monomer species AChR · B* · B (and AChR · B_2^*), initiated by adding an excess of nonlabelled α-bungarotoxin (B), is biphasic suggesting a three state cascade for the B-sites: $R_\alpha \rightarrow R'_\alpha \rightarrow R''_\alpha$ with the exchange dissociation constants: $(k'_{diss})_B = 5.5(\pm 1) \cdot 10^{-5}\ s^{-1}$ and $(k''_{diss})_B = 3(\pm 1) \cdot 10^{-6}\ s^{-1}$ at 293 K. The data are consistent with dissociative intermediate steps of ligand exchange on *two* different interconvertible conformations of *one* binding site. The dissociation of bound B* by excess of the neurotransmitter acetylcholine (ACh) is biphasic. At [ACh] = 0.1 M both B* are released from the AChR · B_2^* species. The mechanism involves associative ternary intermediates (AChR · B*A, AChR · B*A_2 and AChR · $B_2^*A_2$). The equilibrium constants (K_A) and dissociation rate constants (k_{-A}) for ACh in the ternary complex state R'_α and R''_α, respectively, are $K'_A = 1.1 \cdot 10^{-2}$ M and $k'_{-A} = 3 \cdot 10^5\ s^{-1}$ and $K''_A = 7.5 \cdot 10^{-2}$ M and $k''_{-A} = 2 \cdot 10^6\ s^{-1}$. It is of physiological importance that the FCS data indicate that the AChR monomer species (M_r = 290 000), which normally at [ACh] ≤ 1 mM only binds *one* ACh molecule, does bind *two* ACh molecules at [ACh] ≥ 0.1 M.

Keywords: Fluorescence correlation spectroscopy; Acetylcholine receptor; α-Bungarotoxin; Fluctuation kinetics

1. Introduction

The rapid synaptic signal transmission between cholinergic muscle and nerve cells is mediated by the postsynaptic acetylcholine receptor (AChR) system. In many cases and especially in Torpedo fish electrocytes, AChR can be isolated as two species.

* Corresponding authors: concerning AChR, E. Neumann, Bielefeld; concerning FCS, R. Rigler, Stockholm.

SSDI 0301-4622(95)00080-1

Conventional preparation conditions yield a dimer species of molar mass $M_r = 580\,000$. The presence of reducing agents leads to the monomer fragment of $M_r = 290\,000$, consisting of homologous subunits of the stoichiometry $\alpha_2\,\beta\gamma\delta$. The two α-subunits of the monomer species are the predominant targets for the binding of the natural neurotransmitter acetylcholine (ACh; A) and of snake α-toxins, which compete with ACh. See the review [1].

The α-toxins prevent the opening of the AChR channel by blocking the binding of ACh. Only extremely high concentrations (≈ 0.1 M) of ACh lead to the dissociation of tightly bound α-toxins ($\approx 10^{-8}$ M). The α-toxins have proven to be a very useful tool to explore dynamic molecular properties of AChR species. The kinetics of the association of α-toxins with AChR as well as the structural changes coupled to the toxin-binding have been investigated by filter assays of radionucleotide-labelled as well as of fluorophore-marked α-toxins. The questions addressed include (i) Are the two α-sites per monomer species equivalent and independent? (ii) Does the biphasic toxin dissociation kinetics reflect differences in the two α-sites or does it indicate that one α-site exhibits two different conformational states with different affinity for the toxin?

It is shown that the method of fluorescence correlation spectroscopy (FCS) is suited to definitely answer some of the not yet resolved questions. FCS allows one to determine the kinetics of slowly interacting molecules with different translational diffusion coefficients at very low concentrations ($\leqslant 10^{-8}$ M). This new technique of molecule monitoring is applied to characterize the interaction dynamics of tetramethylrhodamin labelled α-bungarotoxin (B*) with the detergent solubilized nicotinic acetylcholine receptor (AChR) of the electric organ of the *Torpedo californica*.

The main physiologically relevant result is that the exchange of bound toxins can proceed via *dissociative* intermediate steps of ligand exchange on two different interconvertible conformations of one binding site. Furthermore, high concentrations of the neurotransmitter ACh (0.1 M) can release both α-toxins from one receptor monomer fragment. Thus at [ACh] $\geqslant 0.1$ M both α-sites of the monomer are occupied by ACh whereas at the physiological level of [ACh] $\leqslant 10^{-3}$ M only one α-site binds ACh [2].

2. Materials and methods

2.1. Acetylcholine receptor (AChR) and α-bungarotoxin (B)

AChR species were isolated as detergent-solubilized dimers and monomers. The receptor proteins were purified by affinity chromatography as described previously [3]. The composition of the standard buffer solution used was 10 mM HEPES (pH 7.4), 100 mM NaCl and 0.5 (wt.-%) of the detergent CHAPS. Tetramethylrhodamin labelled α-bungarotoxin (TMR-α-Btx, abbreviated B*) was commercial (Molecular Probes, Inc., USA). In solution the receptor species are mixed micelle-like ternary complexes of protein, endogeneous lipids and detergents.

2.2. Fluorescence correlation spectroscopy (FCS)

The experimental set up for the FCS measurements was used as described [4]. The species counted by FCS are TMR-α-Btx (B*) and B* bound to the AChR species of varying total (monomer) concentrations ($[R_t] = 1$ nM–1.6 μM), mostly at $[B_t^*] = 40$ nM. For the dissociation kinetics the mixtures of B* and AChR were incubated for a time interval $\geqslant 4$ h before the FCS measurements. Laser excitation wavelength was $\lambda_{ex} = 515$ nm; power 1 mW, channel time unit was $\tau = 0.1$ ms. A droplet of a 10 μl solution was applied to the surface of the objective lens of a microscope through which the laser beam passes. Fluorescence emission was collected by the same objective and the intensity fluctuations were analyzed in terms of an autocorrelation function.

2.3. Analysis of the FCS data

Provided that only one type of species was present, for instance, TMR-α-Btx alone, the analysis of the autocorrelation curve was carried out with a nonlinear least squares' fitting programme using the autocorrelation function [4,5]:

$$G(\tau) = 1 + \frac{1}{N}\left[\frac{1}{1+\tau/\tau_d}\right]\left[\frac{1}{1+\left(\omega_z/\omega_{x,y}\right)^2\tau/\tau_d}\right]^{1/2} \quad (1)$$

where N and τ_d denote the number and the diffusion time constant of the fluorescent particles, respectively, τ is the channel time and ω_z and $\omega_{x,y}$ are the extensions of the Gaussian volume element of observation (laser beam) along the perpendicular to the optical axis, respectively [4]. The quantity $\pi \cdot \omega_{x,y}^2$ is the area covered by the laser beam through which the molecules diffuse; $\omega_{x,y}^2$ is determined by a standard measurement with rhodamine 6G. The beam dimensions and the translational diffusion coefficients D are related by

$$\tau_d = \omega_{x,y}^2/(4D). \quad (2)$$

If in the process of complex formation the dissociation rate constants k_{diss} are large compared with the diffusion time constants τ_d, i.e. $k_{diss}^{-1} < \tau_d$, the analysis of the autocorrelation curves yields the numerical values of N and D of each the interacting species.

The diffusion times of the free TMR-α-Btx molecules (B^*) and of the complexes AChR · B^* and AChR · B_2^* are sufficiently different. Therefore we can use the following autocorrelation function to determine the degree of binding y^* of TMR-α-Btx to the AChR

$$G(\tau) = 1 + \frac{1}{N^*}\left[\frac{(1-y^*)\cdot\theta_f + y^* Q^2 \cdot \theta_b}{[(1-y^*)+y^* Q]^2}\right] \quad (3)$$

where N^* is the total number of free TMR-α-Btx molecules (B^*) and of the receptor species with bound B^*, i.e. the monoliganded form AChR · B^* and the biliganded AChR · B_2^*. The θ-terms are defined by:

$$\theta_f = \frac{1}{1+\tau/\tau_f}\left(\frac{1}{1+(\omega_z/\omega_{x,y})^2\tau/\tau_f}\right)^{1/2}$$

and

$$\theta_b = \frac{1}{1+\tau/\tau_b}\left(\frac{1}{1+(\omega_z/\omega_{x,y})^2\tau/\tau_b}\right)^{1/2}$$

τ_f and τ_b are the diffusion time constants of free (B^*) and bound (B_b^*) toxin molecules, respectively. The factor $Q = q_b/q_f$ is the ratio of the quenching coefficients of B_b^* and B^*, respectively.

The diffusion time constant τ_f of the free B^* is sufficiently different from the time constants τ_b(AChR · B^*) and τ_b(AChR · B_2^*). Because the molar mass of AChR ($M_r \approx 290\,000$) is much larger than that of B^* ($M_r \approx 8000$), the translational diffusion constants of AChR · B^* and AChR · B_2^* are practically equal. Hence we use τ_b(AChR · B^*) = τ_b(AChR · B_2^*). Therefore, in FCS *both* the monoliganded and the biliganded AChR monomers count as *one* type of fluorescent species.

Explicitly, the fraction of FCS bound B^* relative to the total B_t^* is defined by

$$y^* = \frac{[B_b^*]}{[B_t^*]} = \frac{[AChR\cdot B^*] + [AChR\cdot B_2^*]}{[B_t^*]} = y_1^* + y_2^* \quad (4)$$

where y_1^* and y_2^* are the contributions of the mono- and biliganded species, respectively. The molecular-thermodynamic degree of binding of B^* is given by

$$y = \frac{[AChR\cdot B^*] + 2\cdot[AChR\cdot B_2^*]}{[B_t^*]} \quad (5)$$

where $y = y_1^* + 2y_2^*$ and the relationship $0 \leqslant y \leqslant 1$ holds. We see that $y_1 = y_1^*$ and $y \geqslant y^*$.

3. Results

The FCS data in Fig. 1 show that the TMR-α-Btx (B^*) molecule, the monoliganded species AChR · B^* and the dimer receptor species (AChR · B^*)$_2$ exhibit autocorrelation functions consistent with the increasing molar mass of the diffusing particles. The diffusion coefficients evaluated with Eq. 1 are given in Table 1.

In contrast to FCS, conventional static fluorescence titration (SFT) directly yields the degree of bound B^* by

$$y = \frac{[B_b^*]}{[B_t^*]} = \frac{F - F_\infty}{F_0 - F_\infty} = \frac{2[R]}{2[R] + \bar{K}} \quad (6)$$

if the simple reaction scheme

$$AChR_\alpha + B^* \rightleftharpoons AChR_\alpha \cdot B^* \quad (7)$$

applies, where R_α represents one of the two independent binding sites of the AChR monomer R ($M_r = 290\,000$); see the discussion. Note that for the total concentration of the AChR monomer we have $[R_t] = [R_{\alpha,t}]/2$. In Eq. 6, $F_0 = F([R_t] = 0)$ and F_∞ =

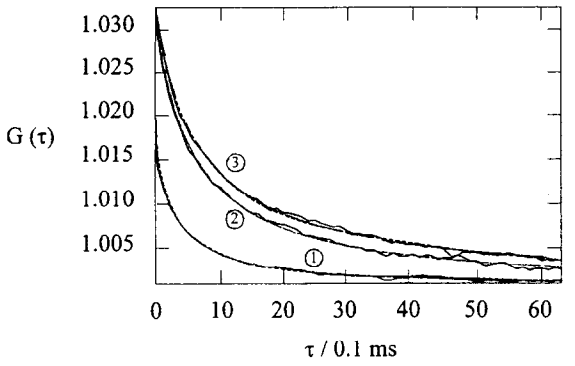

Fig. 1. Fluorescence autocorrelation function $G(\tau)$ as a function of channel time (τ) for the translational diffusion of (1) TMR-α Btx (B^*), (2) monoliganded *Torpedo californica* AChR monomer species ($R \cdot B^*$) and (3) liganded AChR dimer species $(RB^*)_2$. Total concentrations: $[B_t^*] = 40$ nM; AChR monomer $[R_t] = 0.2$ μM (95% monoliganded, RB^*); AChR dimer $[(R_2)_t] = 0.1$ μM (95% monoliganded with respect to a monomeric part R). All species in 0.1 M NaCl, 0.5% (w) CHAPS, 10 mM HEPES, pH 7.4, 293 K (20°C). Excitation wavelength of the laser $\lambda_{ex} = 515$ nm; power 1 mW; 1 channel time unit is $\tau = 0.1$ ms.

$F([R_t] \rightarrow \infty)$ are the fluorescence emission intensity at total AChR concentration zero, $[R_t] = 0$, and at $[R_t] \gg [B_t^*]$, respectively.

For the case of independent 1:1 stoichiometry, the equilibrium constant can be determined from the mass action formalism for Eq. 7 according to:

$$\overline{K} = \frac{1-y}{y}(2[R_t] - y[B_t^*]) = 2[R_t]_{y=0.5} - 0.5[B_t^*] \quad (8)$$

Table 1
Translational diffusion times (τ_D) and diffusion coefficients (D)

Molecule	M_r	τ_D (ms)	$D \cdot 10^{10}$ ($m^2\ s^{-1}$)
Rhodamin 6G	478	0.146	2.8
TMR-α Btx (B^*)	8000	0.4	1.0
AChR B^* (monomer)	350000	1.2	0.33
$(AChR \cdot B^*)_2$ (dimer)	700000	1.4	0.29

FCS solution conditions: 0.1 M NaCl, 0.2 mg lipid/ml (≈ 25 mM), 0.5% CHAPS (w), 10 mM HEPES, pH 7.4; 293 K (20°C). The *Torpedo californica* AChR protein is associated with lipid and detergent. The monomer and dimer species are mixed micelles. The relative molar masses M_r are estimates; using M_r (monomer) = 290000; the contribution of lipid ($M_r \approx 800$) and detergent is estimated to $65 \times 800 = 52000$ [3].

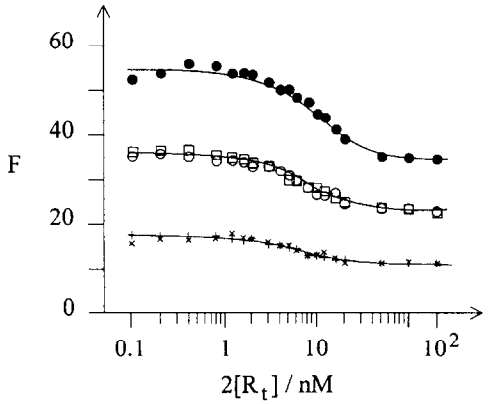

Fig. 2. Static fluorescence titration of TMR-α Btx (B^*) with *Torpedo californica* AChR monomer species. Fluorescence emission (F) in arbitrary units as a function of the total toxin binding site concentration 2 $[R_t]$ (logarithmic scale) for two sets of three different total initial concentrations $[B_t^*] = 5$(x, *), 10 (○, □) and 15 nM (●), respectively; 0.1 M NaCl, 10 mM HEPES, pH 7.4, 293 K (20°C). Excitation $\lambda_{ex} = 554$ nm, emission $\lambda_{em} = 577$ nm. Quantum yield ratio of bound B_b^* to free B^* is given by $Q = q_b/q_f = F_\infty/F_0 = 0.65 \pm 0.05$. The overall equilibrium constant $\overline{K} = [B^*] \cdot 2[R_t]/[B_b^*]$ is estimated from the $[R_t]$ value at $y = 0.5$ according to $\overline{K} = 2[R_t]_{y=0.5} - 0.5\,[B_t^*] = 1.5 \pm 0.5$nM.

where $2[R_t]_{y=0.5} = [R_{\alpha,t}]_{y=0.5}$ is the total α-site concentration at half saturation of binding. Data evaluation of the three titration sets in Fig. 2 in terms of Eqs. 6 and 8 yields $\overline{K} = 1.5 \pm 0.5$ nM. In addition, the titration data provide the quantum yield ratio Q (554/577) for the excitation and emission wavelengths $\lambda_{ex} = 554$ nm and $\lambda_{em} = 577$ nm, respectively:

$$Q = \frac{q_b}{q_f} = \frac{F_\infty}{F_0} = 0.65 \pm 0.05. \quad (9)$$

In Fig. 3, it is seen that in the first 40 min (and also in the longer time range, data not shown) the B^*-binding to AChR is of pseudo-first order with respect to AChR. The values of $[R_t]$ and $[B_t^*]$ are such that the ratio $r = [AChR \cdot B_2^*]/[AChR \cdot B^*] = 1/5$ indicates 83% of the receptor species being in the monoliganded state $AChR \cdot B^*$; see the discussion. The relaxation rate $1/\tau'$ is linearly dependent on $[R_t]$, Fig. 4, suggesting that the association rate coefficient is given by $k'_{ass} \approx 1/\tau'$. Presently we have only applied pseudo-first order conditions for the receptor species. Note that for $[R_t] \gg [B_t^*]$, there are only monoliganded AChR species. The alternative condi-

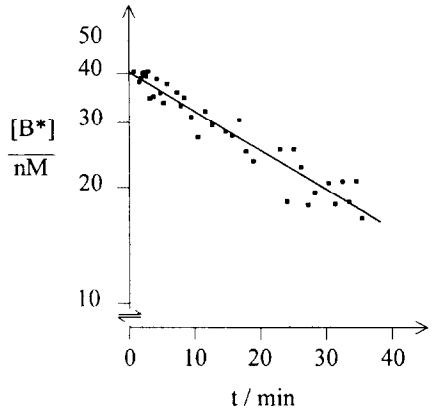

Fig. 3. Association kinetics of TMR-αBtx (B^*) and AChR monomer species. Concentration [B^*] (logarithmic scale) of free B^* as a function of time (t) after addition of B^* to yield [B_t^*] = 40 nM. AChR monomer total concentration [R_t] = 60 nM (total binding site concentration 2[R_t] = 120 nM) 0.1 M NaCl, 0.2 mg lipid/ml, 0.5% (w) CHAPS, 10 mM HEPES, pH 7.4, 293 K (20°C).

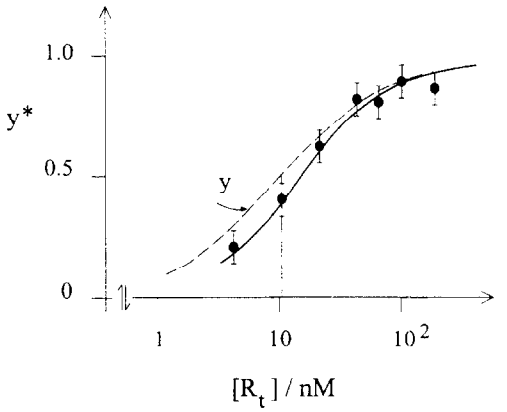

Fig. 5. Degree $y^* = [B_b^*]/[B_t^*]$ of bound TMR-αBtx (B_b^*) as a function of total AChR monomer concentration [R_t]. Since in FCS each complex, AChR·B^* and AChR·B_2^*, count as one species, $y^* = [AChR \cdot B^*]/[B_t^*] + [AChR \cdot B_2^*]/[B_t^*] < y$, with $y = [AChR \cdot B^*]/[B_t^*] + 2[AChR \cdot B_2^*]/[B_t^*]$. Note that at $[R_t] \gg [B_t^*]$, $y^* = y$.

tion $[B_t^*] \gg [R_t]$, faces technical problems of low $G(\tau)$-values because of high fluorophore concentrations.

Fig. 5 shows the results of the FCS titration of a given amount of B^* with increasing concentrations of receptor monomer species. As expected from Eqs. 4 and 5 data evaluation according to Eqs. 6 and 8 shows that $y^* < y$, in particular at low [R_t] values.

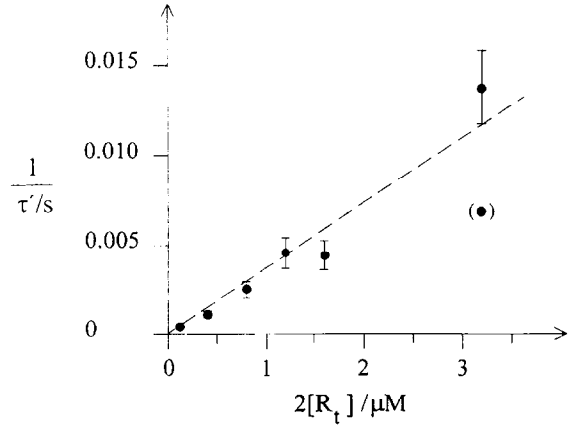

Fig. 4. Reciprocal time constant ($1/\tau'$) of the pseudo-first order association kinetics of TMR-αBtx (B^*) and AChR monomer species as a function of total site concentration (2[R_t]). The slope yields $d(1/\tau')/d(2[R_t]) = k'_{ass} = 3.8(\pm 0.5) \cdot 10^3\ M^{-1}\ s^{-1}$, at 293 K (20°C).

The y-curve was calculated from the simple mass action expression (8) using $\bar{K} = 1$ nM. At $[R_t] \gg [B_t^*]$, where $y = y^* = y_1$, both y and y^* are identical. We see that $\bar{K}$ from FCS is the same as $\bar{K} = 1.5 \pm 0.5$ nM from SFT, Fig. 2.

In Fig. 6 it is evident that the dissociation of B^* from the complexes AChR·B_2^*, enforced by the addition of unlabelled α-Btx (B) to the receptor monomer complexes, proceeds in at least two kinetic phases. The experimental conditions [R_t] = 200 nM are such that at [B_t^*] = 40 nM we expect $y^* = y = y_1 = 1$. The evaluation of y^* with Eq. 3 does not include the small fraction of those B^* molecules from which the TMR-label is hydrolytically removed with time. If this is taken into account, then indeed $y^* = 1$. On the same line, triplet state contributions are not explicitly recorded [6] because they do not interfere on the time scale relevant here. The results of the normal mode analysis in terms of two exponentials (time constants $\tau' = (k'_{diss})_B^{-1}$ and $\tau'' = (k''_{diss})_B^{-1}$ and amplitudes A', A'') are summarized in Table 2. It is noted that the amplitude ratio A'/A'' is the same, independent of the total AChR concentration.

The dissociation of B^* from the complexes AChR·B^* and AChR·B_2^* caused by an excess of the natural neurotransmitter acetylcholine (A) is multiphasic, too. The data are similar to those in Fig. 6

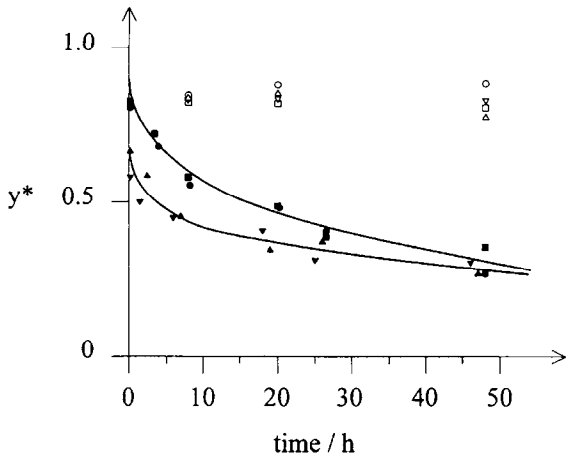

Fig. 6. Dissociation exchange kinetics. The fraction $y^* = [B_b^*]/[B_t^*]$ of bound TMR-αBtx (B_b^*) as a function of time, after addition of unlabelled αBtx (B), $[B_t] = 10$ μM, to a AChR monomer species, incubated for 4 h with $[B_t^*] = 40$ nM, 0.1 M NaCl, 0.2 mg lipid/ml, 0.5% (w) CHAPS, 10 mM HEPES, pH 7.4, 20°C. Open symbols, control at $[B_t] = 0$; ■, ●, two data sets at $[R_t] = 0.2$ μM yielding about 95% monoliganded receptor ($AChR \cdot B^*$); ▲, ▼, two data sets at $[R_t] = 20$ nM yielding about 80% biliganded receptor ($AChR \cdot B_2^*$).

(and are not shown). Due to photo instability of the fluorophore at large measuring times only the first ($1/\tau'$) and second ($1/\tau''$) relaxation phases can be reliably analyzed. We found that $1/\tau'$ linearly increases from $\leqslant 10^{-6}$ s^{-1} to 10^{-5} s^{-1} and $5 \cdot 10^{-4}$ s^{-1} at increasing concentrations of ACh from [A] = 10 μM to 1 mM and 0.1 M, respectively. The slope is $d(1/\tau')/d[A] = 5 \cdot 10^{-3}$ M^{-1} s^{-1}. At [A] = 0.1 M, $1/\tau'' = 4 \cdot 10^{-6}$ s^{-1}, and $d(1/\tau'')/d[A] = 4 \cdot 10^{-5}$ M^{-1} s^{-1}.

Table 2
Relaxation rates ($1/\tau$) and amplitudes (A) of the dissociation exchange kinetics $AChR \cdot B^* + 2B \rightarrow AChR \cdot B_2 + B^*$

$[R_t]$/ nM	$(\tau'/\mu s)^{-1}$	A'	$(\tau'/\mu s)^{-1}$	A''	A'/A''
200	49 ± 24	0.24 ± 0.1	3.7 ± 1.1	0.59 ± 0.1	0.41
20	65 ± 50	0.18 ± 0.1	2.6 ± 1.4	0.44 ± 0.1	0.42

Data evaluation according to $y^* = A' e^{-t/\tau'} + A'' e^{-t/\tau''}$.
At $2[R_t] = 400$ nM the ratio $r = [R \cdot B_2^*]/[RB^*]$ is $r \approx 0.05$, i.e. there is 95% monoliganded AChR. At $2[R_t] = 40$ nM, $r \approx 4$, i.e. there is 80% of the $R \cdot B_2^*$ species. Data analysis (see text) yields $(1/\tau') = (k'_{diss})_B = 5.5(\pm 1) \cdot 10^{-5}$ s^{-1} and $(1/\tau'') = (k''_{diss})_B = 3.0(\pm 1) \cdot 10^{-6}$ s^{-1}.

4. Discussion

Since in FCS mono- and multiliganded receptor macromolecules $AChR \cdot B_n^*$ ($n = 1, 2, ..$) count as only one type of (diffusing) fluorescent species, detailed data analysis is unambiguous only for the AChR monomer with its two α-sites R_α. It is repeated that for the AChR monomer R, the total toxin site concentration is $[R_{\alpha,t}] = 2[R_t]$.

4.1. Association kinetics of TMR-α-Bgt to the AChR

As evident in Fig. 4, the association of B^* to AChR in excess, $[R_t] \gg [B^*]$, is of pseudo-first order. This is in line with observations made for all other α-toxins, labelled or unlabelled [7–11]. The first order relaxation rate for B^*, $1/\tau' \approx k'_{ass} = 3.8 \cdot 10^3$ M^{-1} s^{-1}, is small compared with $1/\tau'$ (B) $\approx k'_{ass}$ (B) $= 2.6 \cdot 10^5$ M^{-1} s^{-1} found for unlabelled α-Bgt (B) [7]. A similar result was found for fluorophor-labelled (CT*) and unlabelled α-cobratoxins (CT); k'_{ass} (CT*) $= 6.7 \cdot 10^3$ M^{-1} s^{-1} for CT* [12] and k'_{ass} (CT) $= 1.3 \cdot 10^5$ M^{-1} s^{-1} for CT [10]. The difference was interpreted in terms of steric hindrance.

If the AChR is solubilized from the electrocyte membranes from the *Torpedo californica*, the in vivo nonequivalent α-sites become equivalent [13]. This observation is in line with the finding that the kinetics of the biliganded $AChR \cdot B_2^*$ is similar to that of the monoliganded species $AChR \cdot B^*$. The data suggest that the solubilized AChR can be described in terms of two independent α-sites. In a mixture of $AChR \cdot B^*$ and $AChR \cdot B_2^*$ the ratio r of bi- and monoliganded species can be calculated from the total concentrations $[B_t^*]$ and $[R_t]$. Substitution of Eq. 5 into Eq. 8 yields

$$r = \frac{[AChR \cdot B_2^*]}{[AChR \cdot B^*]} = \frac{[B_t^*]}{2\overline{K}}(1 - y). \qquad (10)$$

The order of magnitude of $k'_{ass} = 10^3$–10^6 M^{-1} s^{-1} suggests that $1/\tau' \approx k'_{ass}$ cannot reflect a simple bimolecular step $B^* + AChR \rightleftharpoons AChR \cdot B^*$ (expected to have $k_{ass} \approx 10^8$ M^{-1} s^{-1}). An adequate scheme for the data in Fig. 3 must therefore include at least two steps for each α-site R_α:

$$B^* + R_\alpha \overset{(K_1)}{\rightleftharpoons} R_\alpha \cdot B^* \underset{k'_{-1}}{\overset{k'_1}{\rightleftharpoons}} R'_\alpha \cdot B^*. \qquad (11)$$

The results in Fig. 4 suggest that the bimolecular step with the equilibrium constant $K_1 = [B^*] \cdot [R_\alpha]/[R_\alpha \cdot B^*]$ is rapidly coupled to the slower structural change characterized by the equilibrium constant $K_1 = [R_\alpha \cdot B^*]/[R'_\alpha \cdot B^*] = k'_{-1}/k'_1$. Normal mode analysis for this condition yields [14]:

$$\frac{1}{\tau'} = \frac{k'_1 \cdot [R_\alpha]}{[R_\alpha] + K_1} + k'_{-1}. \quad (12)$$

Since $1/\tau'$ is linearly dependent on $[R_t]$, we must assume that $K_1 \gg [R_\alpha]$. This inequality must be valid up to $[R_{\alpha,t}] = 2[R_t] \approx 3$ μM (Fig. 4). Therefore, within the margin of experimental error, K_1 may be at least two orders of magnitude larger than 3 μM. For further estimates we thus assume $K_1 \geqslant 10^{-4}$ M.

The linear dependence of $1/\tau'$ on $[R_t]$, extrapolating to approximately zero (Fig. 4), also suggests that in the receptor concentration range of 1 μM to 3 μM, we can assume that:

$$\frac{k'_1 \cdot [R_\alpha]}{K_1} = \frac{k'_1 \cdot 2[R_t]}{K_1} \gg k'_{-1}. \quad (13)$$

Therefore, for $[R_t] \geqslant 0.2$ μM, Eq. 12 reduces to $(1/\tau') = k'_{ass} \cdot 2[R_t] = k'_1 \cdot [R_{\alpha,t}]/K_1$, where $k'_{ass} = k'_1/K_1 = 3.8 \cdot 10^3$ M^{-1} s^{-1}. From Eq. 13 we obtain $k'_1 = k'_{ass} \cdot K_1 \geqslant 0.38$ s^{-1}, which is a value consistent with a slow conformational transition induced by the binding of B^*.

The experimental conditions of the association kinetics (data in Figs. 3 and 4) are such that one of the two (equivalent) R_α-sites of the receptor monomer is not occupied; see Eq. 10. This situation is different from the binding of unlabelled α-Bgt to $AChR \cdot B^*$ species, where one of the α-sites is already occupied when the other one can bind B.

4.2. Exchange kinetics of B^* versus B

The enormous acceleration of the biphasic dissociation of B^* from the complex $AChR \cdot B^*$ by an excess of unlabelled α-Bgt (B) suggests (i) that at least three interconvertible states for one binding site are involved:

$$R_\alpha \rightleftharpoons R'_\alpha \rightleftharpoons R''_\alpha, \quad (14)$$

and (ii) that the excess of B leads to a direct 'attack' of B on the complexes $R'_\alpha \cdot B^*$ and $R''_\alpha \cdot B^*$. Therefore, the induced fit binding reaction cascade $B^* + R_\alpha \rightleftharpoons R_\alpha \cdot B^* \rightleftharpoons R'_\alpha \cdot B^* \rightleftharpoons R''_\alpha \cdot B^*$ is not reverted by binding of B exclusively to the free sites R_α thereby releasing B^* from the $R_\alpha \cdot B^*$ complex only. Since the kinetics of the direction $R_\alpha \cdot B^* \rightarrow R'_\alpha \cdot B^* \rightarrow R''_\alpha \cdot B^*$ is slow (Fig. 3), such an exchange mechanism would be much slower than is actually observed.

In detail, for the AChR state R'_α we observe the appearance of free B^* according to

$$R'_\alpha \cdot B^* + 2B \overset{(K_1^*)}{\rightleftharpoons} R'_\alpha \cdot B^* B + B \rightleftharpoons R'_\alpha \cdot B_2 + B^* \quad (15)$$

where $K_1^* = [R'_\alpha \cdot B^*] \cdot [B]/[R'_\alpha \cdot B^* B]$ is a dissociation equilibrium constant similar to K_1 discussed in the context of Eq. 11. If $K_1^* \approx K_1 \geqslant 10^{-4}$ M, the first step in Eq. 15 is rapidly coupled to the exchange step:

$$R'_\alpha \cdot B^* B + B \underset{(k'_{ass})_B}{\overset{(k'_{diss})_B}{\rightleftharpoons}} R'_\alpha \cdot B_2 + B^* \ldots. \quad (16)$$

The relaxation rate $1/\tau'$ at $[B] \gg [B^*]$ was found to be independent of [B] (data not shown) suggesting a ligand exchange according to a dissociative mechanism [14]. For instance, reaction (16) involves the two steps:

$$R'_\alpha \cdot B^* \cdot B \underset{(k'_1)_B}{\overset{(k'_{-1})_B}{\rightleftharpoons}} R'_\alpha \cdot B + B^* \quad (17)$$

and

$$R'_\alpha \cdot B + B \underset{k'_-}{\overset{k'_+}{\rightleftharpoons}} R'_\alpha \cdot B_2. \quad (18)$$

The kinetic analysis yields [14]:

$$\frac{1}{\tau'} = (k'_{diss})_B + (k'_{ass})_B \quad (19)$$

where

$$(k'_{diss})_B = \frac{(k'_{-1})_B k'_+ [B]}{k'_+ [B] + (k'_1)_B [B^*]}$$

and

$$(k'_{ass}) = \frac{k'_1 k'_- [B^*]}{k'_+ [B] + k'_1 [B^*]}.$$

The rate constants $(k'_1)_B$ and k'_+ and the equilibrium constants $(K_1)_B = (k'_{-1})_B/(k'_1)_B$ and $K'_\pm = k'_-/k'_+$ both refer to overall bimolecular processes which are similar to the reaction kinetics described by Eq. 11 with $k'_{ass} = k'_1/K_1 = 3.8 \cdot 10^3\ M^{-1}\ s^{-1}$ (Fig. 4 and Eq. 13). We therefore may assume that the approximations $(k'_1)_B \approx k'_+ \approx k'_{ass}$ and $(K_1)_b \approx K'_\pm$ hold true. Because of $[B_t] \gg [B_t^*]$, here $[B_t] = 10\ \mu M$ and $[B_t^*] = 40$ nM, we readily realize that $(k'_{diss})_B \approx (k'_{-1})_B$ and $(k'_{ass})_B \approx (k'_1)_B \cdot K'_\pm \cdot [B^*]/[B]$. As in similar cases of exchange kinetics with large excess of one ligand, here B, the relationship

$$\frac{1}{\tau'} = (k'_{diss})_B = (k'_{-1})_B, \tag{20}$$

applies where the inequality $(k'_{diss})_B \gg (k'_{ass})_B$ is implicit; see Eq. 19. Eq. 20 can be quantitatively justified. Since $(k'_{diss})_B = 5.5 \cdot 10^{-5}\ s^{-1}$ (Table 2), we obtain the approximation $(K'_1) \approx (k'_{diss})_B/k'_{ass} = 1.5 \cdot 10^{-8}$ M and thus $K'_\pm \approx 1.5 \cdot 10^{-8}$ M. Substitution into the expression for $(k'_{ass})_B$ yields $(k'_{ass})_B \approx 2.3 \cdot 10^{-7}\ s^{-1}$. Therefore, indeed $(k'_{ass})_B \ll (k'_{diss})_B$.

Because the slower relaxation mode characterized by $1/\tau''$ is also independent of [B] at $[B_t^*] \ll [B_t]$, similar analysis for the step

$$R''_\alpha \cdot B^* \cdot B + B \underset{(k''_{ass})_B}{\overset{(k''_{diss})_B}{\rightleftharpoons}} R''_\alpha \cdot B_2 + B^* \tag{21}$$

and similar arguments (as for $1/\tau'$) yield:

$$\frac{1}{\tau''} = (k''_{diss})_B = (k''_{-1})_B \tag{22}$$

where $(k''_{diss})_B = 3(\pm 1) \cdot 10^{-6}\ s^{-1}$ (Table 2). Assuming $(k''_1)_B \approx k''_+ \approx k'_{ass}$, we obtain $K''_\pm \approx (K''_1)_B = (k''_{-1})_B/(k''_1)_B \approx (k''_{diss})_B/k'_{ass} \approx 0.8(\pm 1) \cdot 10^{-9}\ M^{-1}$. The comparison with the SFT equilibrium value $\bar{K} = 1.5 \pm 0.5$ nM (Fig. 2) suggests that the final distributions obtained by FCS (Figs. 4 and 6) are indeed the equilibrium values, i.e. $\bar{K} = (K''_1)_B$, indicating the consistency of the data.

In the case of the biliganded AChR · B_2^* species the overall exchange according to

$$AChR \cdot B_2^* + 2B \rightleftharpoons AChR \cdot B_2 + 2B^* \tag{23}$$

is consistently analyzed in terms of two independent binding sites, using the Eqs. 14 to 21. This is in accordance with the observation that the amplitude ratio for mono- and biliganded species, respectively, is the same (Table 2) and that the rate coefficients $(k'_{diss})_B = (k'_{-1})_B = 5.5(\pm 1) \cdot 10^{-5}\ s^{-1}$ and $(k''_{diss})_B = (k''_{-1})_B = 3(\pm 1) \cdot 10^{-6}\ s^{-1}$ are also the same within the margin of error, supporting the equivalence and independence of the two α-sites in the solubilized AChR monomer species.

4.3. Release of bound B* by excess of A

The data analysis shows that the exchange of the big ligand B* by the small agonist molecule A according to the overall process:

$$AChR \cdot B^* + A \underset{k_{ass}}{\overset{k_{diss}}{\rightleftharpoons}} AChR \cdot A + B^* \tag{24}$$

is actually a cascade:

$$AChR \cdot B^* + A \underset{k_{-A}}{\overset{k_A}{\rightleftharpoons}} AChR \cdot B^* \cdot A \underset{(k_1)^*}{\overset{(k_{-1})^*}{\rightleftharpoons}} AChR \cdot A + B^*, \tag{25}$$

involving the intermediate ternary complex AChR · B* · A where both B* and A are on or near one α-site (R_α) of the AChR monomer.

Because of $[A] \gg [B^*]$, the exchange of B* by A is enormously accelerated. It involves directly the states $R_\alpha \cdot B^*$, $R'_\alpha \cdot B^*$ and $R''_\alpha \cdot B^*$ as in the case of the exchange of B* by B. The analysis of the two exchange levels (biphasic relaxation curves) which were measured yields [14]:

$$\frac{1}{\tau'} = k'_{diss} = \frac{k'_A \cdot (k'_{-1})^*}{k'_{-A} + (k'_{-1})^*}[A] \tag{26}$$

and

$$\frac{1}{\tau''} = k''_{diss} = \frac{k''_A \cdot (k''_{-1})^*}{k''_{-A} + (k''_{-1})^*}[A] \tag{27}$$

because in both cases the data suggest that the inequality $k_{diss} \gg k_{ass}$ holds. The rate constants $(k_{-1})^*$ for the dissociation of B* in Eq. 25 refer to similar processes as the rate constants k_{-1} for the dissociation of B* in Eqs. 18 and 22. Therefore we set

$$(k'_{-1})^* = (k'_{-1})_B \text{ and } (k''_{-1})^* = (k''_{-1})_B.$$

The rate constants k'_{-A} and k''_{-A} reflect the normally rapid dissociation of a small ligand from a ternary encounter complex [12]. It is therefore very likely that $k_{-A} \gg (k_{-1})^*$ holds for all three receptor states to be considered, see Eq. 14.

The linear dependencies of the relaxation rates $1/\tau'$ and of $1/\tau''$ as a function of [A] yield, respectively,

$$\frac{1/\tau'}{[A]} = \frac{k'_A \cdot (k'_{-1})_B}{k'_{-A} + (k'_{-1})_B} \approx \frac{(k'_{-1})_B}{K'_A} \qquad (28)$$

and

$$\frac{1/\tau''}{[A]} = \frac{k''_A \cdot (k''_{-1})_B}{k''_{-A} + (k''_{-1})_B} \approx \frac{(k''_{-1})_B}{K''_A}. \qquad (29)$$

If we insert the experimental data $(1/\tau')/[A] = 5 \cdot 10^{-3}$ M^{-1} s^{-1} and $(k'_{-1})_B = 5.5 \cdot 10^{-5}$ s^{-1} into Eq. 28 and $(1/\tau'')/[A] = 4 \cdot 10^{-5}$ M^{-1} s^{-1} and $(k''_{-1})_B = 3 \cdot 10^{-6}$ s^{-1} into Eq. 29, we obtain $K'_A = 1.1 \cdot 10^{-2}$ M and $K''_A = 7.5 \cdot 10^{-2}$ M.

In the reaction Eq. 25 k_A is the association rate constant. If the R_α-site occupied by B^* does not change the affinity of the second R_α-site of the AChR monomer species, we assume for the two receptor states R'_α and R''_α that $k'_A = k''_A \approx 2.4 \cdot 10^7$ M^{-1} s^{-1} [15]. Since generally $K_A = k_{-A}/k_A$, we estimate that $k'_{-A} = k'_A \cdot K'_A \approx 3 \cdot 10^5$ s^{-1} and that $k''_{-A} = k''_A \cdot K''_A \approx 2 \cdot 10^6$ s^{-1}. These values are consistent with the assumption that $k_{-A} \gg (k_{-1})^*$ used previously holds true.

In summary, in contrast to the exchange of bound B^* by B showing a dissociative mechanism, the small molecules A replace the bound B^* via an associative mechanism. The same result was found with other α-toxins [10].

It is interesting to note that at (unphysiologically) high concentrations of ACh, both toxin molecules are replaced by A

$$AChR \cdot B_2^* + 2A \rightleftharpoons AChR \cdot A_2 + 2B^*.$$

Therefore the FCS data suggest that the AChR monomer binds two ACh molecules provided the concentration of A is high enough. Physiologically, the monomer part of the native AChR dimer binds only one ACh molecule [2], but two α-toxins.

Acknowledgements

We gratefully acknowledge an EMBO grant to B.R. and financial support by the Deutsche Forschungsgemeinschaft, grant SFB 223/C01 to E.N. as well as grants from the Swedish Technical Research Council, the K. and A. Wallenberg Foundation and the J. and L. Grönberg Foundation to R.R..

References

[1] A. Karlin, Exploration of the nicotinic acetylcholine receptor, Harvey Lectures, 85 (1991) 71–107.

[2] H.W. Chang, E. Bock and E. Neumann, Long-lived metastable states and hysteresis in the binding of acetylcholine to *Torpedo californica* acetylcholine receptor, Biochemistry, 23 (1984) 4546–4556.

[3] T. Schürholz, J. Kehne, A. Gieselmann and E. Neumann, Functional reconstitution of the nicotinic acetylcholine receptor by CHAPS dialysis depends on the concentration of salt, lipid and protein, Biochemistry, 31 (1992) 5067–5077.

[4] R. Rigler, U. Mets, J. Widengren and P. Kask, Fluorescence correlation spectroscopy with high count rate and low background: analysis of translational diffusion, Eur. Biophys. J., 22 (1993) 169–175.

[5] R. Rigler, J. Widengren and U. Mets, Interactions and kinetics of single molecules as observed by fluorescence correlation spectroscopy, in O.S. Wolfbeis (Editor), Fluorescence Spectroscopy, Springer-Verlag, Berlin, 1992, pp. 13–24.

[6] J. Widengren, R. Rigler and U. Mets, Triplet-state monitoring by fluorescence correlation spectroscopy, J. Fluoresc., 4 (1994) 255–258.

[7] T. Endo, M. Nakanishi, S. Furukawa, F.J. Joubert, N. Tamiya and K. Hayashi, Stopped-flow fluorescence studies on binding kinetics of neurotoxins with acetylcholine receptor, Biochemistry, 25 (1986) 395–404.

[8] S.G. Blanchard, U. Quast, K. Reed, T. Lee, M.I. Schimerlik, R. Vandlen, T. Claudio, C.D. Strader, H.-P.H. Moore and M.A. Raftery, Interaction of [^{125}I]-α-bungarotoxin with acetylcholine receptor from *Torpedo californica*, Biochemistry, 18 (1979) 1875–1883.

[9] R.J. Lukas, H. Morimoto, M.R. Hanley and E.L. Bennett, Radiolabeled α-bungarotoxin derivatives: kinetic interaction with nicotinic acetylcholine receptors, Biochemistry, 20 (1981) 7373–7378.

[10] A. Maelicke, B.W. Fulpius, R.P. Klett and E. Reich, Acetylcholine receptor responses to drug binding, J. Biol. Chem., 252 (1977) 4811–4830.

[11] G. Weiland, B. Georgia, V.T. Wee, C.F. Chignell and P.

Taylor, Ligand interaction with cholinergic receptor-enriched membranes from *Torpedo*: influence of agonist exposure on receptor properties, Mol. Pharmacol., 12 (1976) 1091–1105.

[12] S. Kang and A. Maelicke, Fluorescein isothiocyanate-labeled α-cobratoxin: Biochemical characterization and interaction with acetylcholine receptor from *Electrophorus electricus*, J. Biol. Chem., 256 (1980) 7326–7332.

[13] B.M. Conti-Tronconi, F. Tang, S. Walgrave and W. Gallagher, Nonequivalence of α-bungarotoxin binding sites in the native nicotinic receptor molecule, Biochemistry, 29 (1990) 1046–1054.

[14] M. Eigen and L. DeMaeyer, Relaxation methods, in S.L. Friess, E.S. Lewis and A. Weissberger (Editors), Techniques of Organic Chemistry, Vol. 8(2), Wiley, New York, 1963, pp. 895–1054.

[15] E. Neumann and H.W. Chang, Dynamic properties of isolated acetylcholine receptor protein: kinetics of the binding of acetylcholine and Ca ions, Proc. Natl. Acad. Sci. USA, 73 (1976) 3994–3998.